

FOUR-DIMENSIONAL LOCAL BOUNDARY SURFACES OF AN ISOTROPICALLY CONSOLIDATED LOOSE SAND

SATORU SHIBUYAⁱ⁾, D. W. HIGHTⁱⁱ⁾ and R. J. JARDINEⁱⁱⁱ⁾

ABSTRACT

Undrained anisotropy, together with the undrained response to monotonic as well as cyclic rotation of principal stress directions, of an isotropically consolidated loose Ham River sand has been investigated by performing three series of hollow cylinder tests. The initial anisotropy of the sand when subjected to a single consolidation pressure was successfully established in the first series of tests, each using different, but fixed in each test, values of α (i.e., the direction of major principal stress relative to the vertical deposition direction) at different b values (i.e., the relative magnitude of intermediate principal stress). The response against monotonic principal stress rotation was also examined in the second series of tests, in which the total stress path defined using the shear stress, t , and α was varied in various manner with b fixed at 0.5. In the third series of tests, the response to cyclic changes of both α and b was examined, and the results were interpreted with the comparative behaviour of the monotonic loading tests with different combinations of α and b . It was found that the sand's undrained anisotropy and cyclic response could be interpreted by invoking the concept of undrained local boundary surface (LBS). The four-dimensional LBS could be visualized in (t, p', α) space as a family of superimposed three-dimensional shapes with different b values.

Key words: anisotropy, effective stress, intermediate stress, principal stress rotation, sand, strength (IGC: D6)

INTRODUCTION

Granular materials exhibit anisotropy in the stress-strain and strength characteristics (Arthur and Menzies, 1972; Oda, 1972 among others). The anisotropic behaviour is also affected by the relative magnitude of intermediate principal stress (Lam and Tatsuoka, 1988). This paper is concerned with the mechanical anisotropy, together with the effects of intermediate principal stress, σ'_2 , of a standard test sand (Ham River Sand, or HRS) when it is loose and sheared under undrained conditions. The experiments described were performed by Shibuya (1985) in a Hollow Cylinder Apparatus (HCA) at Imperial College, London. This apparatus, which is described by Hight et al., (1983), is equipped with local strain sensors and can subject relatively large samples (254 mm outside diameter, 203 mm inside diameter, 254 mm height) to generalized stress conditions, including continuous rotation of the major principal stress axis direction with respect to the vertical, α . It allows the sensitivity of soils to loading direction (anisotropy) and relative intermediate principal stress magnitude to be examined. We report here the behaviour seen in tests on isotropically consolidated loose sand, including the effects of changing σ'_2 . The results are interpreted by referring to the concept

of a four-dimensional (4-D) Local Boundary Surface (LBS).

CONCEPT OF LOCAL BOUNDARY SURFACE (LBS)

It seems widely accepted that the concept of three-dimensional state boundary surface defined in (e, p', t) space for the mechanical behaviour of cohesive soils cannot be straightforwardly applicable to the behaviour of sand. Two obvious reasons for this are; i) unlike clays, the $e-p'$ curve in consolidation does not collapse onto a unique relationship, but depends on the initial density at deposition, and ii) the $e-\log p'$ relationship cannot be simulated by using a straight line. Accordingly, the void ratio of sand as a state parameter may be properly understood to be 'local' by considering possible variations of the initial density at deposition as well as the pressure level during both consolidation and shearing. The terminology of Local Boundary Surface (LBS) was first employed by Zdravkovic and Jardine (2000). The LBS concept originated from the finding by Gens (1982, 1985) that the effective stress paths followed during triaxial tests on normally consolidated samples of a single reconstituted clay did not collapse onto a unique State Boundary Surface (SBS) when normalized by the Horslev equiva-

ⁱ⁾ Associate Professor, Graduate School of Engineering, Hokkaido University, Sapporo Japan; formerly Research Assistant, Imperial College of Science, Technology and Medicine, London, U.K.

ⁱⁱ⁾ Director, Geotechnical Consulting Group, London, U.K., also Visiting Professor at Imperial College London.

ⁱⁱⁱ⁾ Professor, Department of Civil and Environmental Engineering, Imperial College, London, U.K.

Manuscript was received for review on January 23, 2002.

Written discussions on this paper should be submitted before November 1, 2003 to the Japanese Geotechnical Society, Sugayama Bldg. 4F, Kanda Awaji-cho 2-23, Chiyoda-ku, Tokyo 101-0063, Japan. Upon request the closing date may be extended one month.

lent pressure: instead the paths depended on the effective stress conditions under which the samples had been consolidated and sheared. Each LBS was defined by the effective stress ratio experienced during virgin consolidation, and formed a surface which undrained effective stress paths subjected to monotonic or cyclic loading could not cross. Drained tests could cross the LBS and progress, in normalized effective stress space, towards the State Boundary Surface (SBS). A similar observation had been made for the behaviour of sand by Tatsuoka (1972).

Under triaxial conditions, the effective stress paths of undrained compression and extension tests (conducted at overconsolidation ratio, $OCR = 1$) mapped out a Local Boundary Surface whose shape varied systematically with the effective stress ratio, K , applied during consolidation. However, each LBS limited the effective stress space that could be occupied by samples consolidated in a particular way after being swelled back to $OCRs > 1.0$. When the samples are sheared under undrained conditions, the effective stress paths of overconsolidated samples turned as they approached the LBS and then conformed with the surface as they were sheared to larger strains. In a similar way, the LBS provided a boundary to the effective stress paths that can be followed during undrained cyclic loading tests (for example, see Hight et al., 1983; Symes et al., 1984).

Jardine (1992) proposed the term LBS and noted that the mechanical behaviour within the surface was (i) largely in-elastic and non-linear, and (ii) controlled by nested

kinematic yield surfaces. Jardine et al. (2001) discuss these latter aspects in more detail, including the anisotropy of Ham River Sand at very small strains, drawing on the work of Kuwano (1999). The envelope to the full family of LBSs (defined by consolidating samples to all possible K ratios and plotting their positions in normalised effective stress space) defined the true outer State Boundary Surface (SBS). Normally consolidated samples could move from one LBS to another by following drained compression paths that led to a different stress ratio (t/p'), noting the shear stress, $t = (\sigma'_1 - \sigma'_3)/2$ and the mean effective stress, $p' = (\sigma'_1 + \sigma'_2 + \sigma'_3)/3$. Zdravkovic and Jardine (2000) invoked the LBS ideas to interpret families of HCA and triaxial tests on a silt, showing that the LBS developed under K_0 conditions is highly anisotropic.

Earlier HCA tests on water-pluviated HRS (Symes et al., 1984, 1988; Shibuya and Hight, 1987) showed that even isotropically consolidated sand could be strongly anisotropic at moderate strains. Drained tests in which t increased while p' and α were held constant (with $b = (\sigma'_2 - \sigma'_3)/(\sigma'_1 - \sigma'_3)$ fixed at 0.5) yielded the stress-strain and strength behaviour that depended strongly on the direction of σ'_1 . HRS samples were less stiff, more contractant and weaker in shear at higher α values. Also the total volumetric strains developed in moving to a particular final stress condition (t, p', α) were practically independent of the stage at which α was rotated. The same was true of the changes in p' induced by moving to a par-

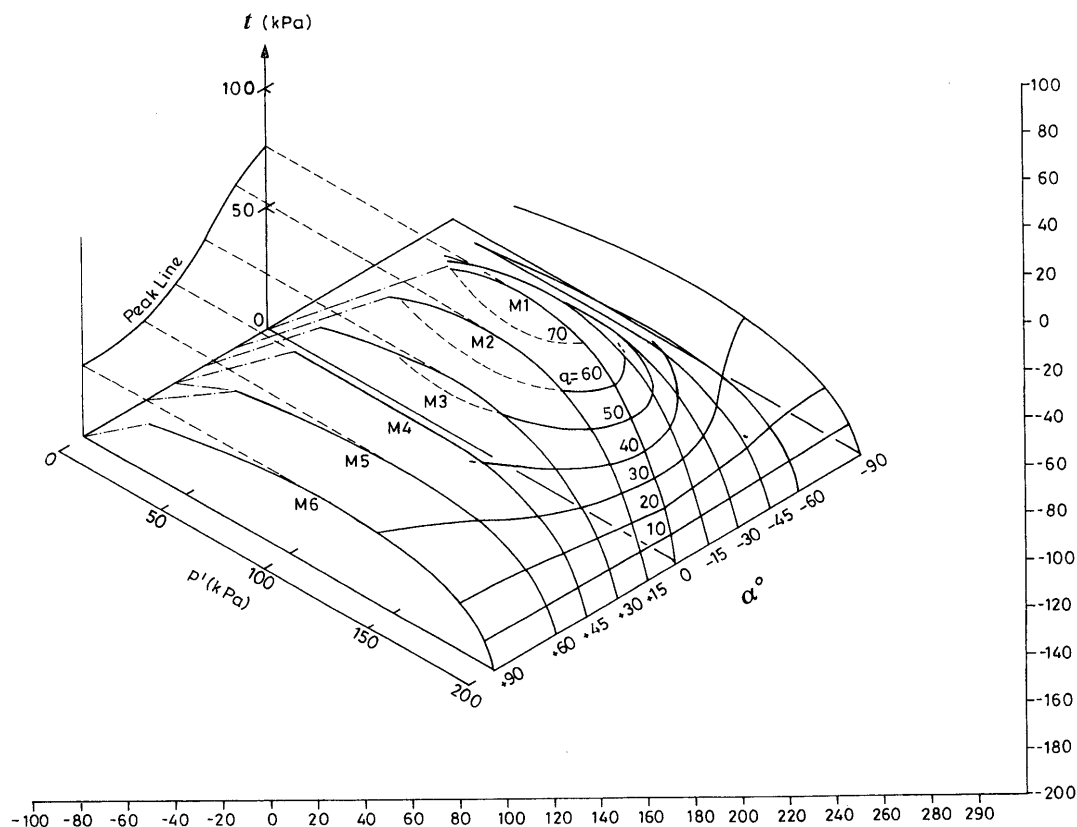


Fig. 1. Local Boundary Surface (LBS) of isotropically consolidated loose Ham River sand at $b = 0.5$ (reproduction of Fig. 1 of Shibuya and Hight, 1987)

ticular (t, α) point under undrained conditions. It was concluded that the sand's shearing response could be described (at least at moderate strains) by a three dimensional (3-D) boundary surface. As seen in Fig. 1, this surface would now be termed the LBS applying to isotropically consolidated specimens, for $b=0.5$.

While all of the undrained tests described above involved fixing b at 0.5 during shear, it is known that b influences the stress-strain and strength relationships of most sands (see for example Yamada and Ishihara, 1979). We describe below suites of additional monotonic

undrained shearing tests which involved changes in both b and α . The role of the now four dimensional (q, p', b, α) LBS in defining undrained response to these more complex stress changes was tested further by experiments where both of b and α were cycled.

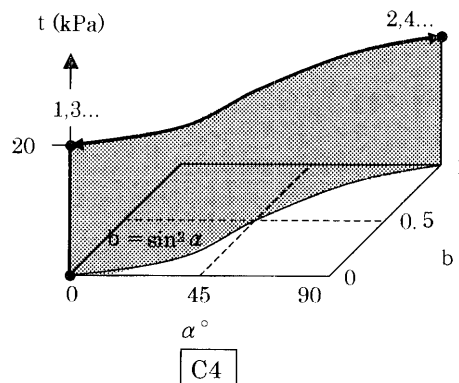
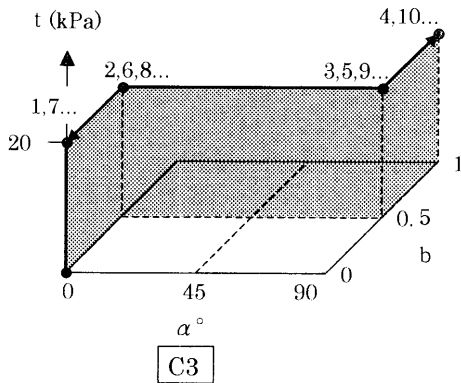
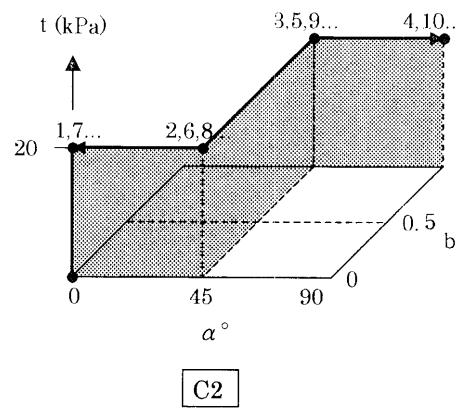
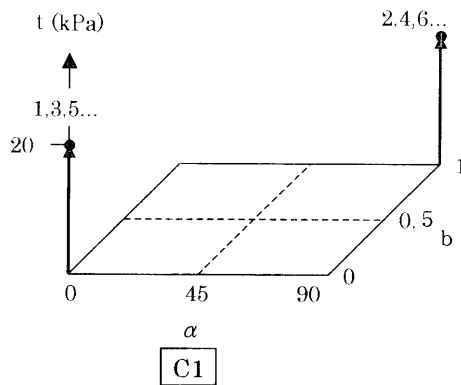
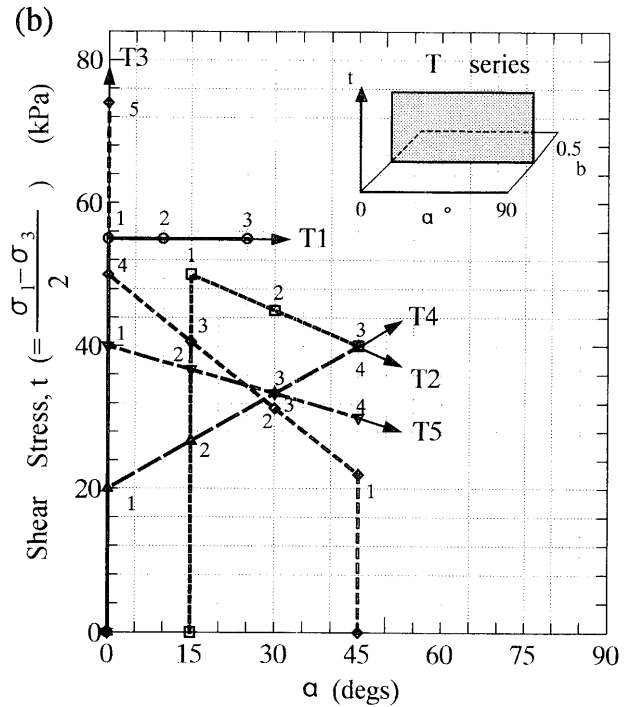
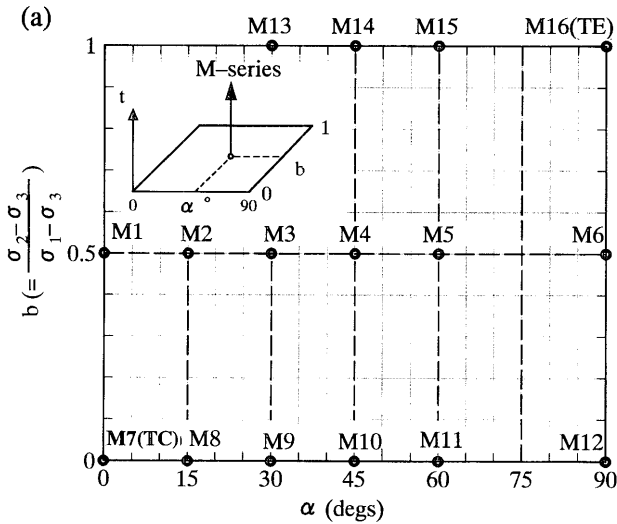


Fig. 2. Total stress paths applied: (a) M-series, (b) T-series and (c) C-series

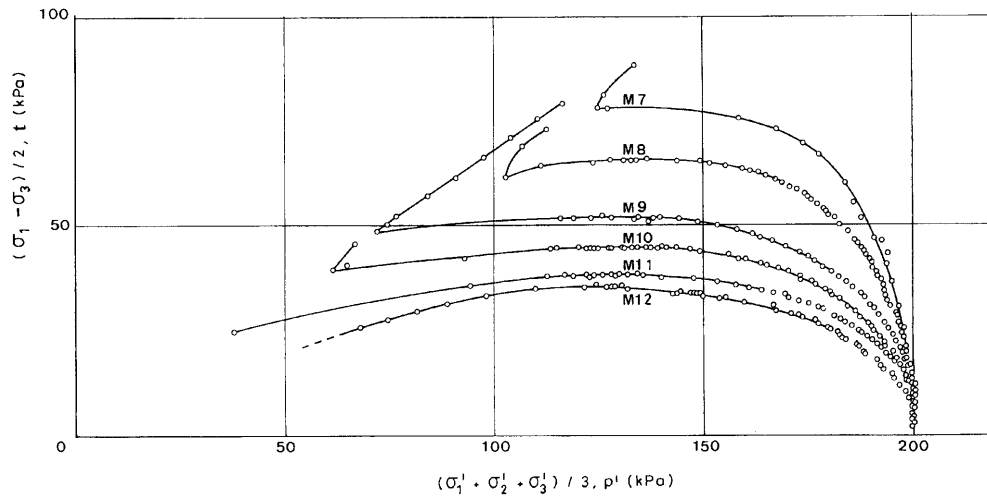


Fig. 3. Undrained effective stress paths for M-series tests at $b=0$

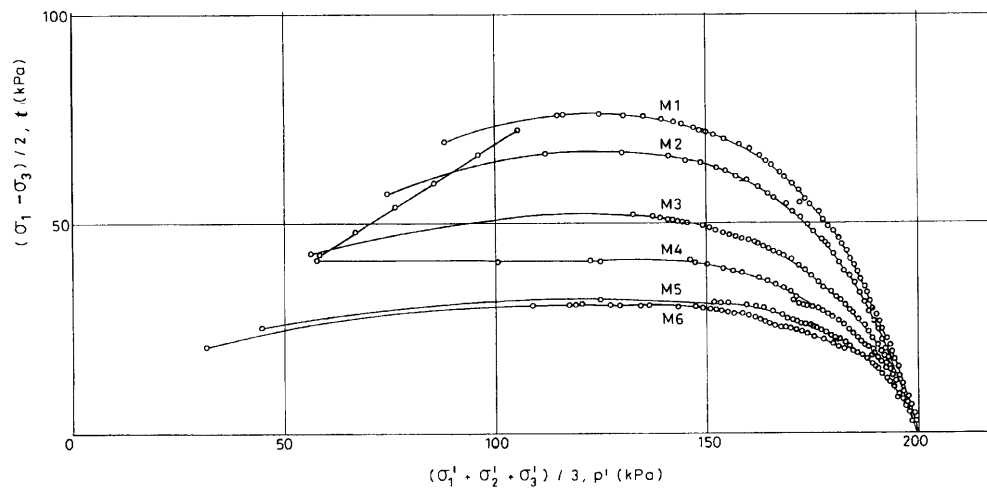


Fig. 4. Undrained effective stress paths for M-series tests at $b=0.5$

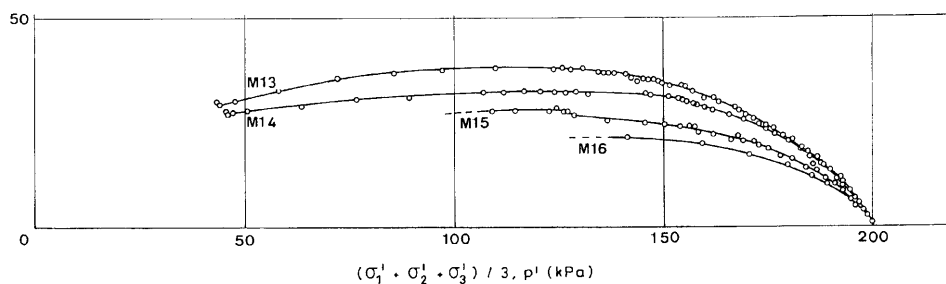


Fig. 5. Undrained effective stress paths for M-series tests at $b=1.0$

DESCRIPTION OF TESTS

The material and sample preparation techniques were identical to those described by Symes et al. (1984, 1988). Loose Ham river sand was selected for the experiments, following Hight et al. (1983) and Shibuya and Hight (1987). Gentle raining through de-aired water led to an initial void ratio of about 0.79 (at a suction of -30 kPa),

matching a relative density of around 25%. The specimens were isotropically consolidated to a mean effective stress, p'_0 , equal to 200 kPa, while maintaining a back pressure of 200 kPa. The pore pressure coefficient, B was in excess of 0.98. Definitions for the average stresses and strains, and descriptions of the local strain measuring instrumentation are given by Hight et al. (1983) and Symes and Burland (1984).

The tests were conducted under stress-control, using a computer-based servo control system (Shibuya, 1988). During the undrained shear stages of each test, the total mean principal stress, p , was kept at a constant value of 600 kPa. Pre-determined loading paths (defined in terms of t , b and α) were followed by incremental adjustments to the axial load, torque, internal and external chamber pressures. A pause period was allowed after achieving each increment of loading so that the specimen could achieve a satisfactory degree of deformation and pore pressure equilibrium (Shibuya, 1988).

As described below, the experiments presented in this paper may be classified into three groups: the M, T and C Series.

M-Series: Establishing the Initial Undrained Anisotropy at Different b -Values

The series M-tests involved undrained shearing with the shear stress, t , being increased monotonically up to failure. During undrained shearing in each test, the b and α values were both maintained constant. As illustrated in Fig. 2(a), sixteen tests were performed, with α varying between 0° and 90° and b between 0 and 1.0, to cover the full range of combinations (excluding the so-called 'no-go' zone, where non-uniformities of radial and circumferential stresses reach unacceptable levels as defined by Hight et al., 1983).

Tests, M7 ($b=0$ and $\alpha=0^\circ$) and M16 ($b=1$ and $\alpha=90^\circ$), correspond to triaxial compression and extension respectively, while M4 ($b=0.5$ and $\alpha=45^\circ$) is equivalent to a standard torsional shear test, in which the shear stress on the horizontal plane $\tau_{z\theta}$ is applied monotonically to an isotropically consolidated sample.

T-Series: Checking the Shape of Local Boundary Surface (LBS)

The value of performing additional tests in which α is rotated during shear, while either holding t constant at some level, or varying t simultaneously with α has been discussed by Shibuya and Hight (1987). In this paper, we consider five experiments, T1 to T5. As illustrated in Fig. 2(b), the undrained shearing stages of these tests started by following the same paths as the constant α M-Series experiments M1, M2 or M4 (all with $b=0.5$), but moved away (at the points marked 1) to follow different paths in the t - α plane. The objective was to define experimentally (in the t - α plane) the gradients of the three dimensional LBS (that applying to loose water-pluviated HRS isotropically consolidated to 200 kPa and sheared undrained keeping $b=0.5$).

C-Series: Probing the LBS by Undrained Cyclic Changes of t , b and α

Four cyclic tests (C1-C4) were undertaken in which t , α and b were varied to first assess the relative sensitivity of the observed response to each parameter, and secondly examine whether the same LBS applied as under monotonic conditions. The cyclic paths illustrated in Fig. 2(c), show how the LBS was probed under fully 4-D stress

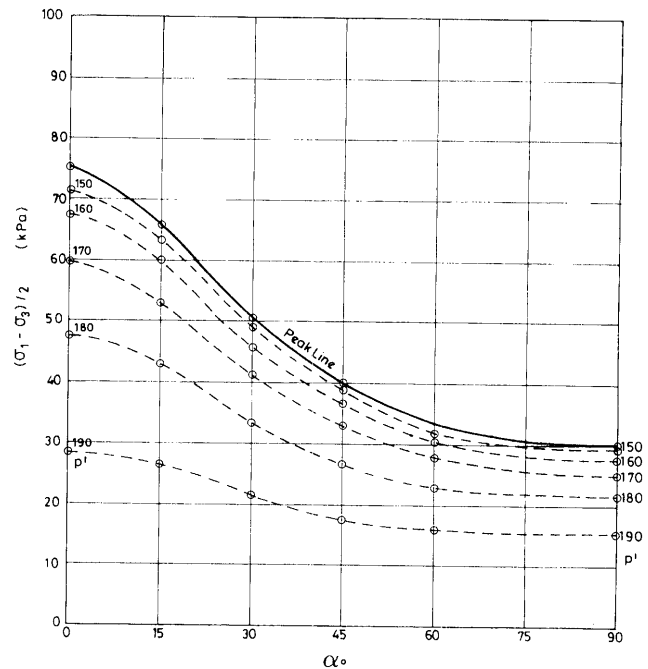


Fig. 6. Projection of a LBS at $b=0.5$ in (t, α) space

conditions. Test C1 corresponded to two-way (compression-extension) cyclic triaxial loading under with the cyclic shear stress amplitude of 20 kPa. In the companion tests, C2, C3 and C4 involved cycling between the two same extreme t , b and α points ($t=20$ kPa, $b=0$, $\alpha=0^\circ$ and $t=20$ kPa, $b=1.0$, $\alpha=90^\circ$) but following three different paths that kept t constant at 20 kPa. Test C4 involved keeping the inner and outer cell pressures equal throughout shear, giving rise to the relationship $b = \sin^2 \alpha$. Note that the stage numbers marked at points where the total stress paths changed direction are indicated to help readers follow the tests.

PRESENTATION AND DISCUSSIONS OF TEST RESULTS

The run-away behaviour was a characteristic feature of loose sand when subjected to undrained monotonic as well as cyclic shear in a stress-controlled apparatus; that is, the specimen exhibits a form of softening in the stress-strain relationship. The phenomenological aspect of the run-away is that, on reaching the peak, the specimen shows abrupt increases of positive pore pressure and strains during which any attempt to control stresses are not rewarded, unless the post-peak behaviour of the material is precisely predicted. In case of the behaviour under cyclic loading, the sudden increases of both pore pressure and strains could practically be considered as 'partial liquefaction'. Since the sand's deformation observed in the pre-peak region was small with strains less than 0.5%, the response of pore pressure, examinations into individual strain components resulted little in clarifying the nature of anisotropic stress-strain behaviour due to limitations involved with the current strain

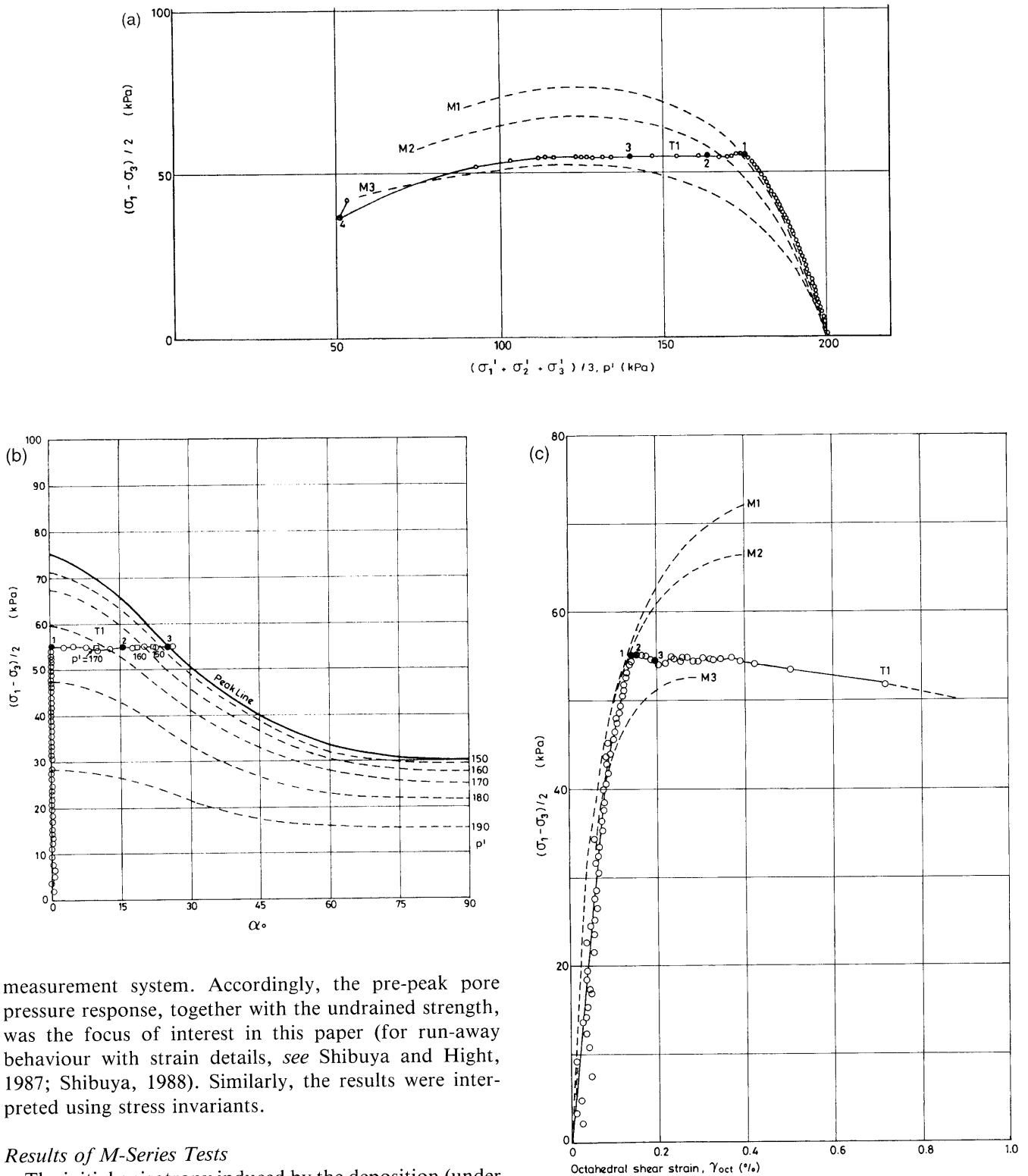


Fig. 7. Undrained effective stress paths and shear strain behaviour for test T1

measurement system. Accordingly, the pre-peak pore pressure response, together with the undrained strength, was the focus of interest in this paper (for run-away behaviour with strain details, see Shibuya and Hight, 1987; Shibuya, 1988). Similarly, the results were interpreted using stress invariants.

Results of M-Series Tests

The initial anisotropy induced by the deposition (under gravity by water-pluviation) combined with isotropic consolidation to 200 kPa is reflected in the effective stress paths followed during the shearing stages of the M-series tests. The paths observed in the 16 tests conducted at b values of 0, 0.5 and 1.0 are plotted in Figs. 3, 4 and 5 respectively, using $t-p'$ co-ordinates.

As already described by Shibuya and Hight (1987), the loose sand exhibited a type of run-away behaviour when sheared monotonically under stress control. On reaching a peak shear stress, t_p , the samples tended to strain

rapidly and undergo continuous reductions in p' up to a point where a quasi-steady state was reached, and the pore pressures and shear strains stabilized. This point corresponds to the Phase Transformation Point (PTP) defined by Ishihara et al. (1975), which distinguishes between the contractant and dilatant phases of behaviour.

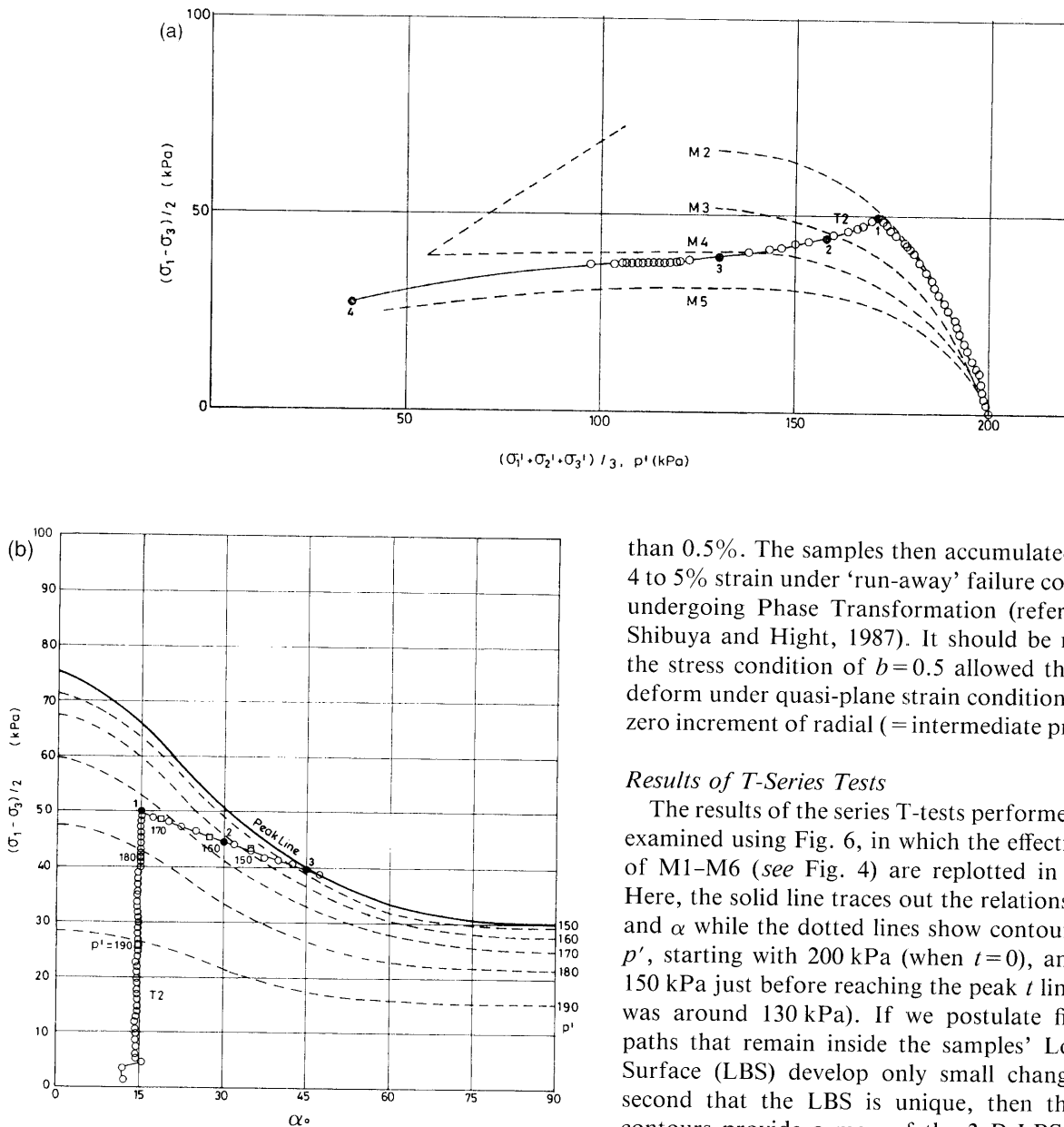


Fig. 8. Undrained effective stress paths for test T2

Pore pressures start to develop negative increments if undrained shearing continues beyond the PTP and samples may then harden through suppressed dilation. It should be mentioned that the final effective stress conditions shown in Figs. 3, 4 and 5 mainly reflect the points at which the sample geometry became excessively non-uniform, rather than any ultimate stage of the material behaviour.

Additional points to note from the M-series tests are:

- (i) The $\alpha = 0^\circ$ tests showed the steepest pre-peak effective stress paths, and
- (ii) t_p was highest at $\alpha = 0^\circ$, dropping rapidly as α increased.

As typically seen in a series of tests (with $b = 0.5$), the shear stress develops a peak value, t_p , in the contractant phase involved with the octahedral shear strain, γ_{oct} less

than 0.5%. The samples then accumulated an additional 4 to 5% strain under 'run-away' failure conditions before undergoing Phase Transformation (refer to Fig. 10 of Shibuya and Hight, 1987). It should be mentioned that the stress condition of $b = 0.5$ allowed the specimens to deform under quasi-plane strain conditions with virtually zero increment of radial (= intermediate principal) strain.

Results of T-Series Tests

The results of the series T-tests performed at $b = 0.5$ are examined using Fig. 6, in which the effective stress paths of M1-M6 (see Fig. 4) are replotted in the t - α plane. Here, the solid line traces out the relationship between t_p and α while the dotted lines show contours for constant p' , starting with 200 kPa (when $t = 0$), and dropping to 150 kPa just before reaching the peak t line (on which p' was around 130 kPa). If we postulate first that stress paths that remain inside the samples' Local Boundary Surface (LBS) develop only small changes in p' , and second that the LBS is unique, then the constant p' contours provide a map of the 3-D LBS for $b = 0.5$, a hypothesis which can be checked by the T-tests outlined below.

The T-series experiments tested whether the 3-D LBS established by the undrained M-series tests (performed at $b = 0.5$) was unique. They also clarified its shape. As shown in Figs. 7 to 11, the imposed t - α stress paths are plotted against the framework given by Fig. 6. The values of p' developed at various stages are annotated, for comparison with the constant p' contours from the M-Series, together with the t_p - α curve. Any path that runs parallel to or below a $p' = \text{constant}$ contour should not involve any further changes in p' . A path directed more steeply (higher $dt/d\alpha$) than the nearest contour would constitute 'loading', while one directed at a lower $dt/d\alpha$ would lead to 'unloading'.

The first point to note is that those portions of the T-Series tests that were common with experiments M1, M2, M4 showed near coincidence in their constant α loading effective stress paths and stress-strain curves: the experimental repeatability was good. However, more

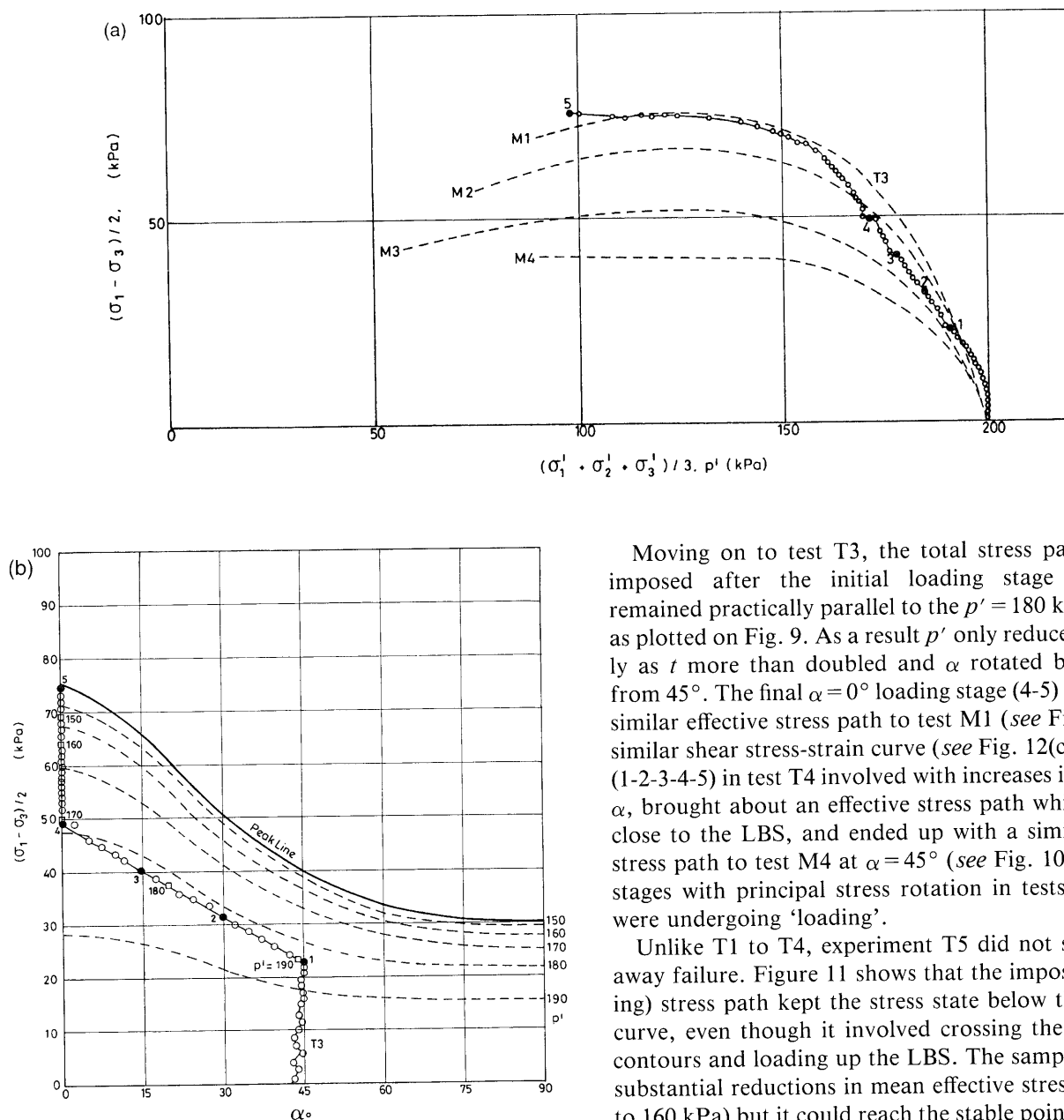


Fig. 9. Undrained effective stress paths for test T3

interesting patterns emerge from the later stages of each test.

When the principal stress direction is rotated in T1, the effective stress path migrated by generating positive pore pressures: the path (1-2-3) travelling close to the p' contours of the comparative M-series tests (see Fig. 7). Considering T2, it can be seen in Fig. 8 that while the total stress path (1-2-3) imposed after the constant α stage involved reducing t , the gradient $\Delta t / \Delta \alpha$ of the nearest constant p' contours were still more negative, and so the path in fact involved remaining on the LBS, crossing the p' contours, and approaching the peak t curve. The samples of tests T1 and T2 were therefore undergoing 'loading', and underwent a run-away failure when they reached the peak-line.

Moving on to test T3, the total stress path (1-2-3-4) imposed after the initial loading stage at $\alpha = 45^\circ$ remained practically parallel to the $p' = 180$ kPa contour, as plotted on Fig. 9. As a result p' only reduced marginally as t more than doubled and α rotated back to zero from 45° . The final $\alpha = 0^\circ$ loading stage (4-5) led to a very similar effective stress path to test M1 (see Fig. 9), and a similar shear stress-strain curve (see Fig. 12(c)). The path (1-2-3-4-5) in test T4 involved with increases in both t and α , brought about an effective stress path which travelled close to the LBS, and ended up with a similar effective stress path to test M4 at $\alpha = 45^\circ$ (see Fig. 10). Again, the stages with principal stress rotation in tests T1 and T2 were undergoing 'loading'.

Unlike T1 to T4, experiment T5 did not suffer a run-away failure. Figure 11 shows that the imposed (t reducing) stress path kept the stress state below the peak t - α curve, even though it involved crossing the constant p' contours and loading up the LBS. The sample developed substantial reductions in mean effective stress (p' falling to 160 kPa) but it could reach the stable point '5' without its octahedral small shear strain exceeding 0.1%. The p' values observed as the path travelled from '1' to '5' were marginally lower than might be expected from the M Series constant p' contours.

Taken together, the T-Series tests confirm that the 3-D LBS does not depend on the route followed by undrained tests. The LBS provides a stable reference surface whose co-ordinates are practically stress-path independent. It should be mentioned that the behaviour occurred in the contractant region involved with generation of small shear strain less than 0.5% as typically seen in Fig. 7(c) for the case of T1. Furthermore, the loading portion of the 3-D LBS may be mapped out in t - α space by contours of constant p' , as shown by the M-series tests. An extra dimension can be added by considering the effects of changing the fourth stress parameter, b .

Results of C-Series Tests

As summarised in Fig. 4, the C-series of tests all cycled

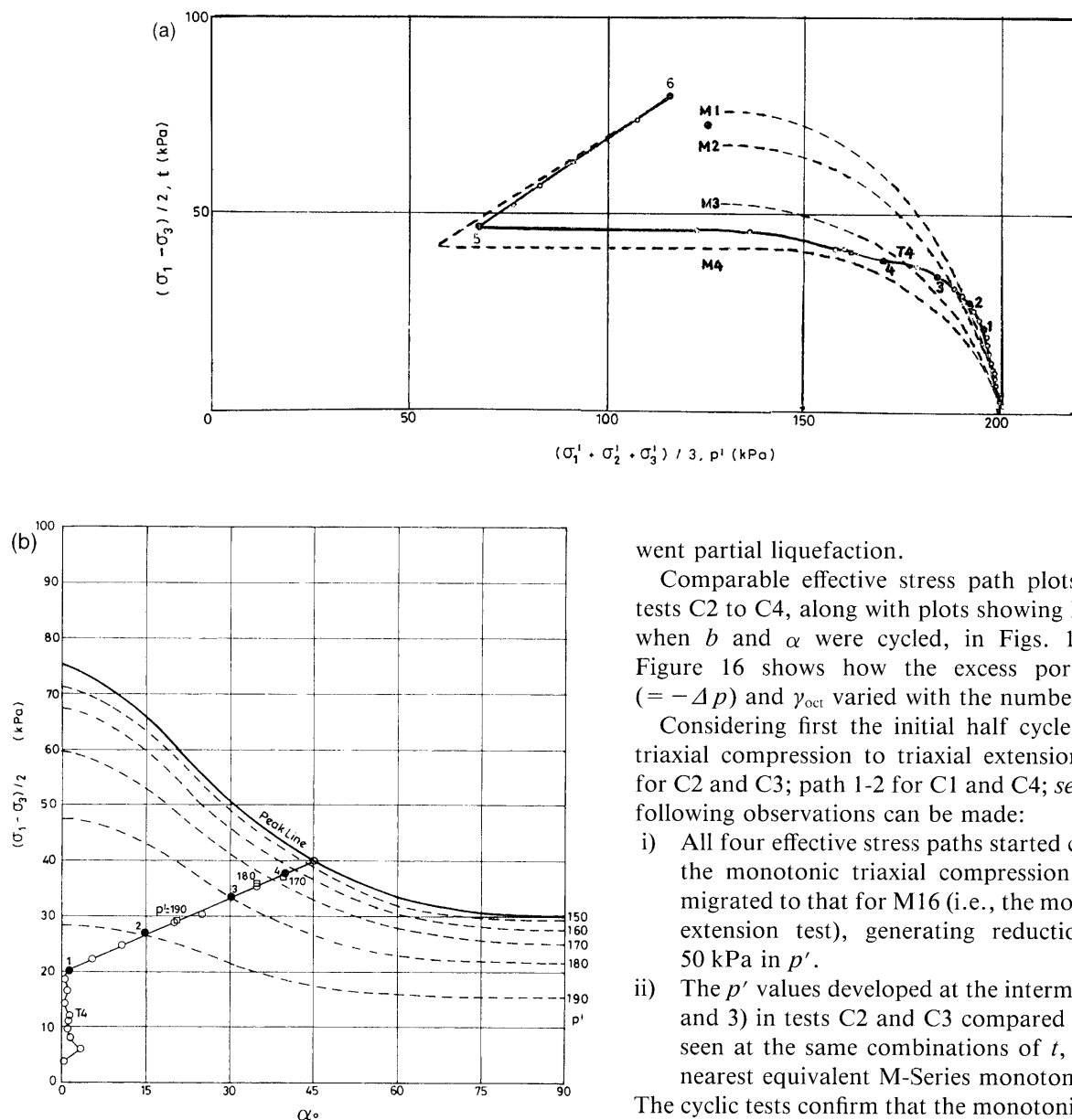


Fig. 10. Undrained effective stress paths for test T4

between the extreme limits of $t = 20$ kPa in triaxial compression with $b = 0$ and $\alpha = 0^\circ$ and $t = 20$ kPa in triaxial extension with $b = 1$ and $\alpha = 90^\circ$. However, each of the four tests followed a different route in the b - α plane, revealing the effects of changing b independently of α .

The effective stress path developed in C1, the conventional cyclic triaxial compression-extension test (performed in the HCA), is shown in Fig. 12, which also displays the paths followed by the monotonic HCA triaxial compression and extension tests (M7 and M16). The role that these monotonic tests play in defining the sand's LBS is clear: the primary loading portions of the cyclic test conform with the monotonic LBS and each cycle develops an incremental reduction in p' that pushes the stress points progressively to the left. The descending portion of the LBS corresponding to the monotonic test M16 also defined the point at which the cyclic test under-

went partial liquefaction.

Comparable effective stress path plots are given for tests C2 to C4, along with plots showing how p' reduced when b and α were cycled, in Figs. 13, 14 and 15. Figure 16 shows how the excess pore pressure Δu ($= -\Delta p$) and γ_{oct} varied with the number of cycles, N .

Considering first the initial half cycle, shifting from triaxial compression to triaxial extension (path 1-2-3-4 for C2 and C3; path 1-2 for C1 and C4; see Fig. 2(c)), the following observations can be made:

- All four effective stress paths started close to that for the monotonic triaxial compression test M7, then migrated to that for M16 (i.e., the monotonic triaxial extension test), generating reductions of around 50 kPa in p' .
- The p' values developed at the intermediate points (2 and 3) in tests C2 and C3 compared well with those seen at the same combinations of t , b and α in the nearest equivalent M-Series monotonic tests.

The cyclic tests confirm that the monotonic loading effective stress paths define a stable four-dimensional LBS. The following features were observed as cycling continued:

- Excess pore pressure was successively accumulated, and p' reduced, as N increased.
- In three tests C2, C3 and C4, partial liquefaction occurred in the fifth cycle, whereas it took place in the sixth cycle in test C1 (i.e., conventional cyclic triaxial test), by showing abrupt increase of γ_{oct} in extension.
- The trends shown in Fig. 16 indicate broadly similar trends between the pore pressures and shear strains accumulated in the four tests. However, the path imposed in test C2 appeared to lead to a given degree of damage occurring at a significantly earlier stage.
- When the changes in b and α were separated in test C2 and C3, the main part of the (irrecoverable) p' reductions and shear strains developed during the α rotation stages. The changes in b had less impact especially when the effective stress was well inside the 4-D LBS as observed in test C2 (see Fig. 13(c)).

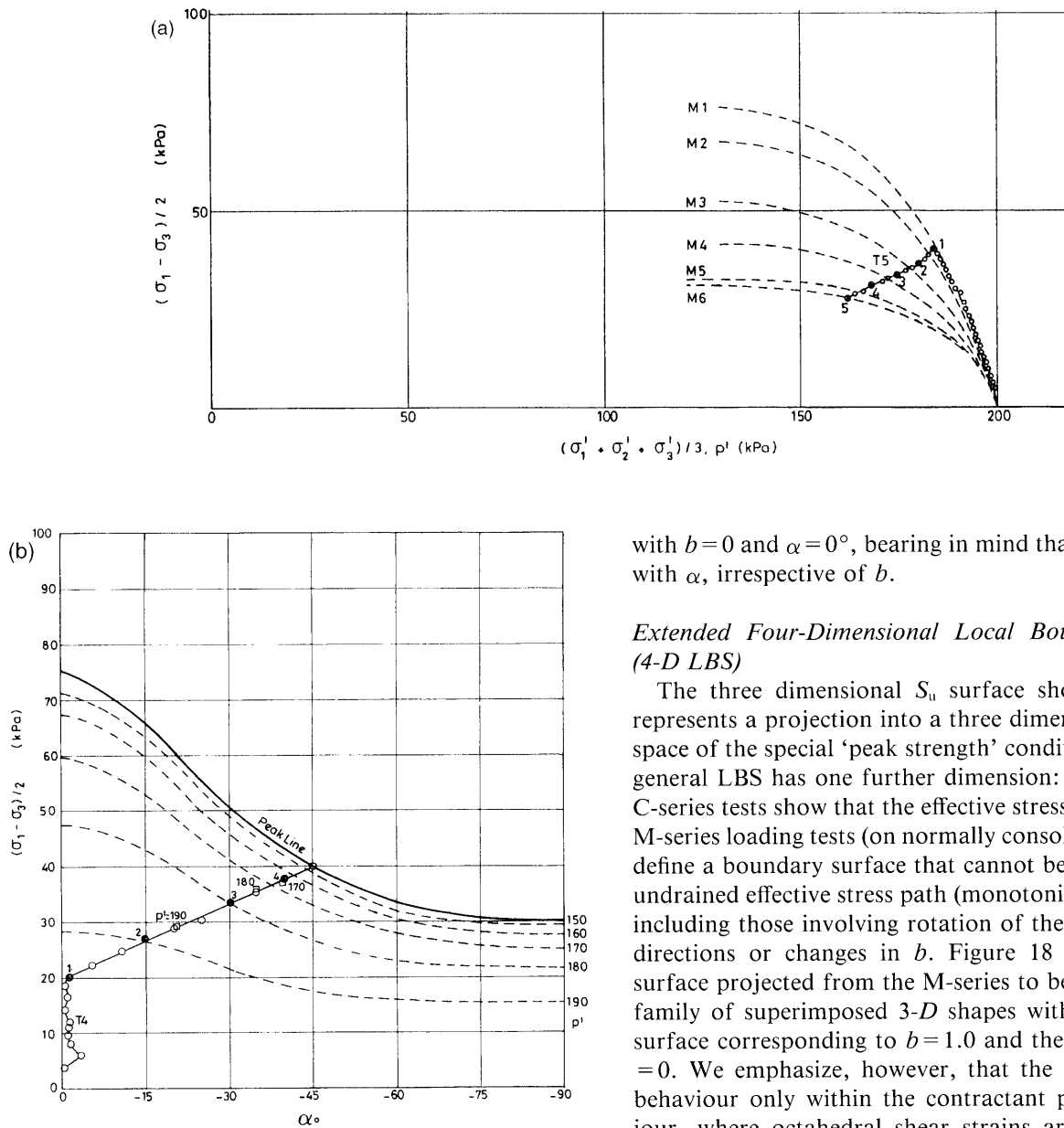


Fig. 11. Undrained effective stress paths for test T5

Undrained Peak Strength-Effects of b and α

The maximum shear stress mobilized in the contractant region (i.e., prior to PT) in the M-series tests may be considered as an undrained shear strength, $S_u (= t_p)$ for the very loose sand. The variations of S_u with b and α are plotted on Fig. 17. The 3D surface obtained after isotropic consolidation to 200 kPa is strongly affected by α , and also influenced by the b -value, noting that the quasi ‘plane strain’ compression with $b=0.5$ and $\alpha=0^\circ$ exhibited the highest value of S_u . The special cases associated with conventional laboratory tests (triaxial compression and extension, and simple shear) are identified on the 3-D S_u surface. The shape of the surface can be idealized by mathematical fitting, so that the peak strength for any arbitrary combination of b and α can be projected in an appropriate way from a routine triaxial compression test

with $b=0$ and $\alpha=0^\circ$, bearing in mind that the S_u reduces with α , irrespective of b .

Extended Four-Dimensional Local Boundary Surface (4-D LBS)

The three dimensional S_u surface shown in Fig. 17 represents a projection into a three dimensional (t, b, α) space of the special ‘peak strength’ conditions. The more general LBS has one further dimension: p' . The T- and C-series tests show that the effective stress paths from the M-series loading tests (on normally consolidated samples) define a boundary surface that cannot be crossed by any undrained effective stress path (monotonic or slow cyclic) including those involving rotation of the principal stress directions or changes in b . Figure 18 allows the 4-D surface projected from the M-series to be visualized as a family of superimposed 3-D shapes with the innermost surface corresponding to $b=1.0$ and the outermost to $b=0$. We emphasize, however, that the surfaces govern behaviour only within the contractant phase of behaviour, where octahedral shear strains are generally less than 1%. Also, the shapes of the LBS are likely to change with initial void ratio, consolidation mean effective stress level, and the style of consolidation.

Establishing and visualizing the LBS shapes allows us to reconsider and redefine the meaning of loading and unloading paths under 3-D or 4-D stress conditions. A loading path can now be understood as being one that first involves the effective stress path state travelling on or close to the LBS, even though t may be reducing. Secondly, the path direction may be either stable or potentially unstable, depending on whether the path moves towards or away from the local maximum in t ($= S_u$). Also, in 2D plots representing constant b conditions, loading tests are those whose stress path gradient, $\Delta t / \Delta \alpha$, match or exceed those of the constant p' contours projected from the LBS. On the other hand, if an imposed increase or decrease of t involves $\Delta t / \Delta \alpha$ falling below that of the nearest constant p' contour, the effective stress path will move back inside the LBS following an unloading path that develops (under monotonic condi-

LOCAL BOUNDARY SURFACE

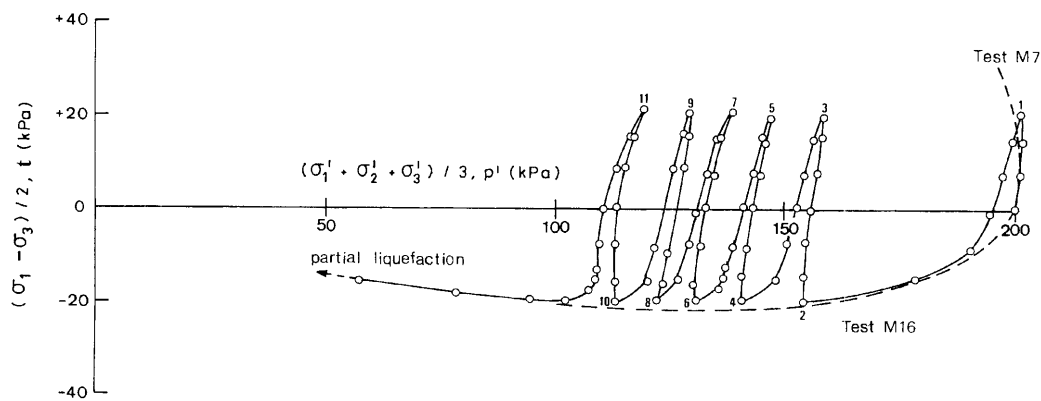


Fig. 12. Undrained effective stress paths for test C1 (triaxial compression-extension test)

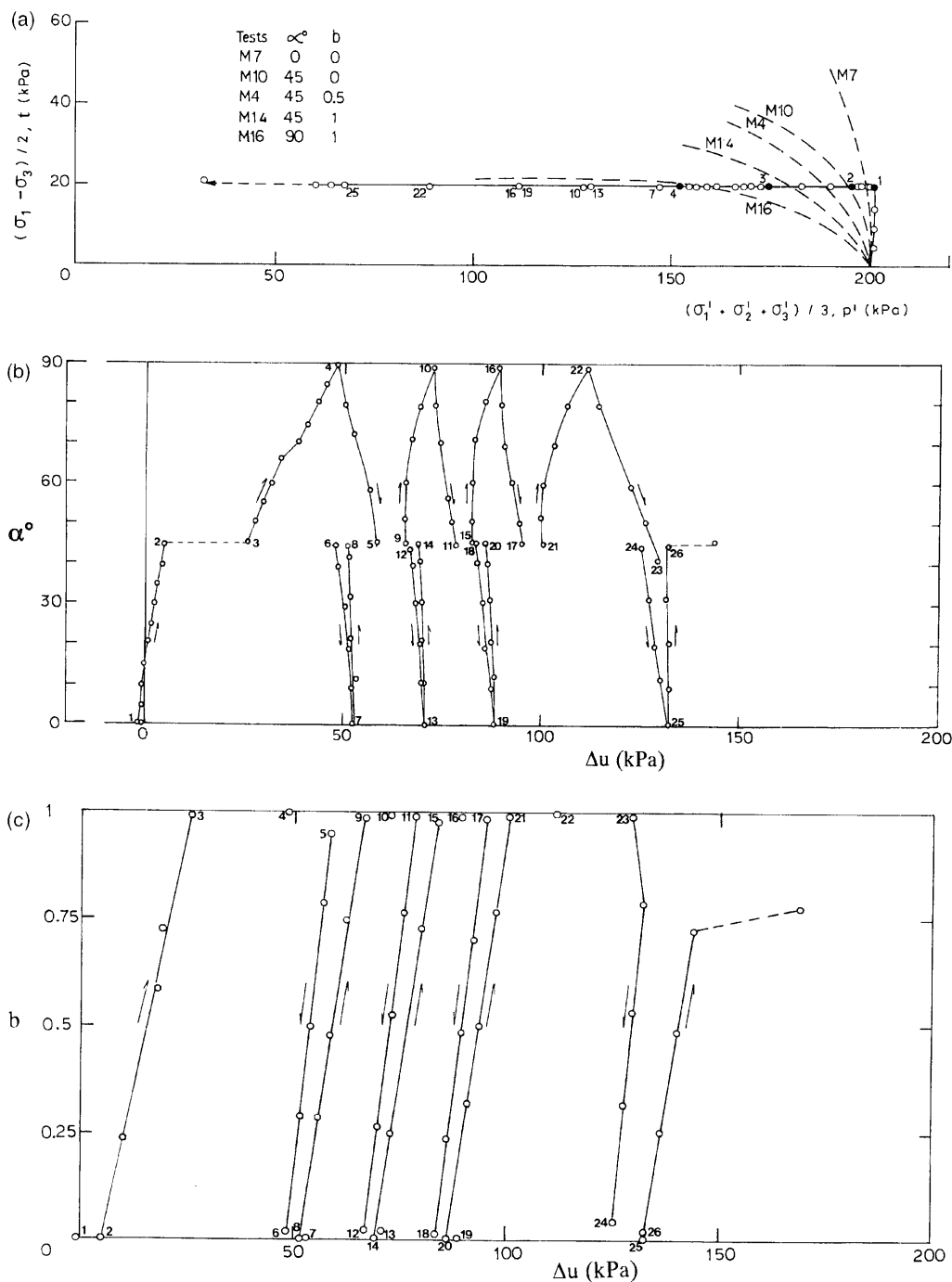


Fig. 13. Undrained effective stress path and excess pore pressure response of test C2

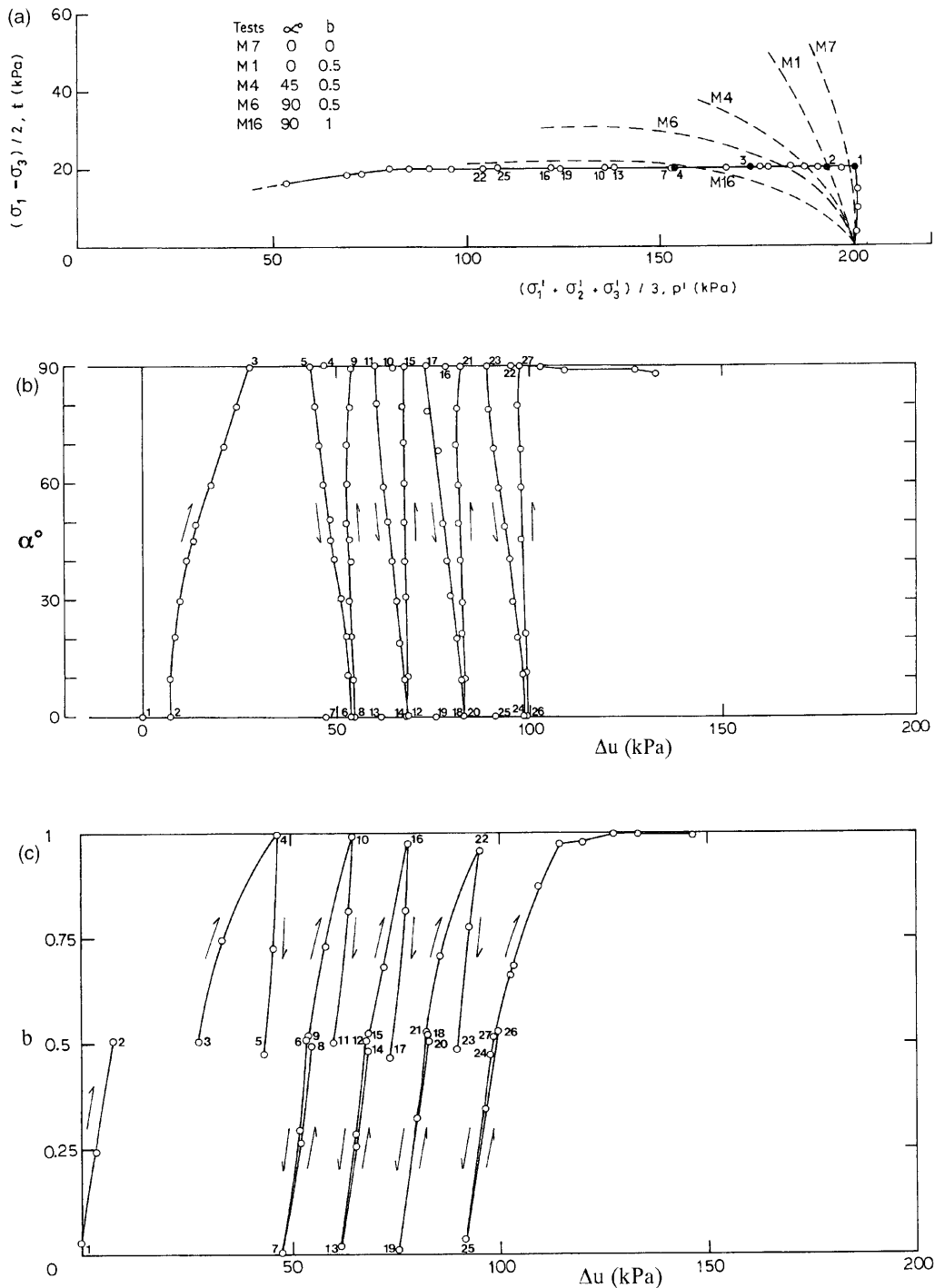


Fig. 14. Undrained effective stress path and excess pore pressure response of test C3

tions) relatively small changes in p' . Repeated cycling within the LBS does lead to larger reductions in p' in the case of loose sand.

As already discussed by Symes et al. (1984, 1988) and Shibuya and Hight (1997), the concept of LBS may be applicable conditionally to the small-strain behaviour of sand samples showing very strong initial anisotropy, for example those prepared by pluviation method. In such samples, the stress-strain and strength behaviour is strongly affected by α as shown in Fig. 18. The effects of any additional anisotropy induced by principal stress

rotation and/or changes in b -value may be muted by showing that the volumetric strain or pore pressure under conditions of drained or undrained shear develops in a manner of being as if independent of the total stress path applied. Care should be taken for the other aspect where the induced anisotropy of sand is significant on the stress-strain behaviour as the sample is sheared on the initially isotropic plane (Arthur and Dunstan, 1977).

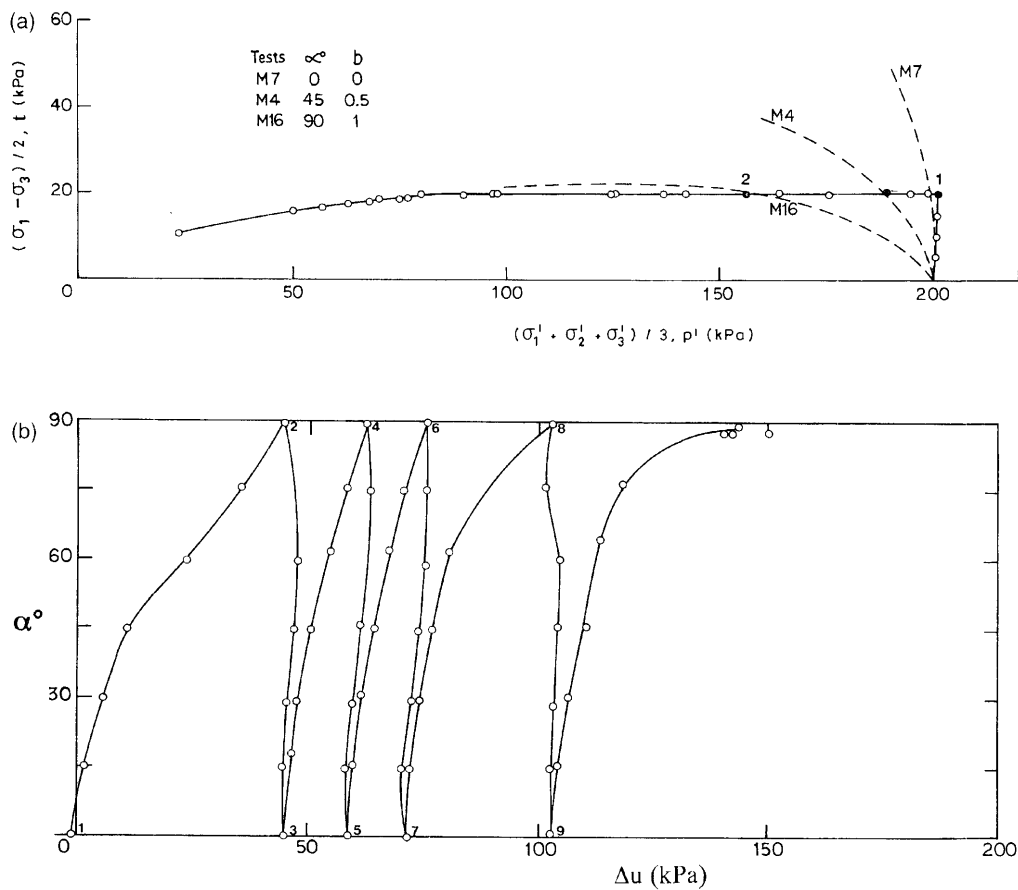


Fig. 15. Undrained effective stress path and excess pore pressure response of test C4

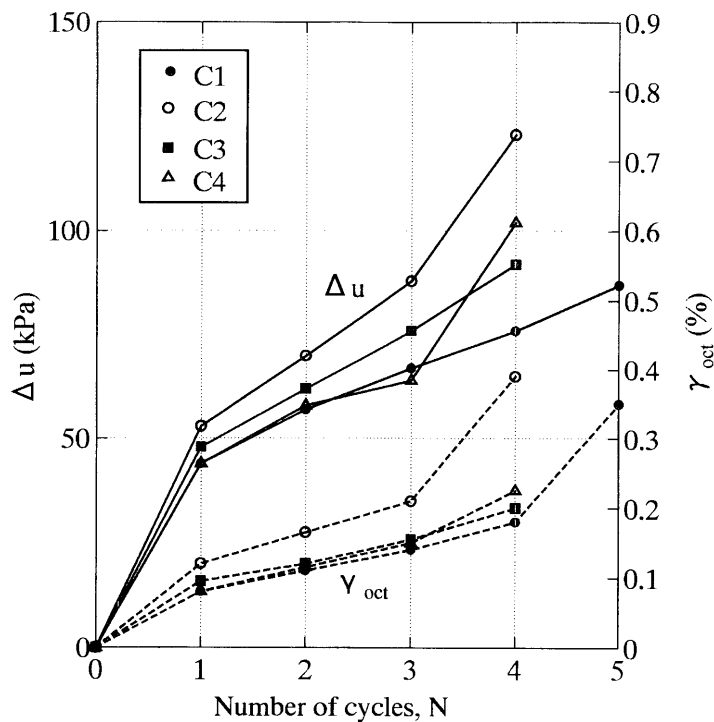


Fig. 16. Accumulated excess pore pressure and octahedral shear strain against number of cycles for tests C1-C4

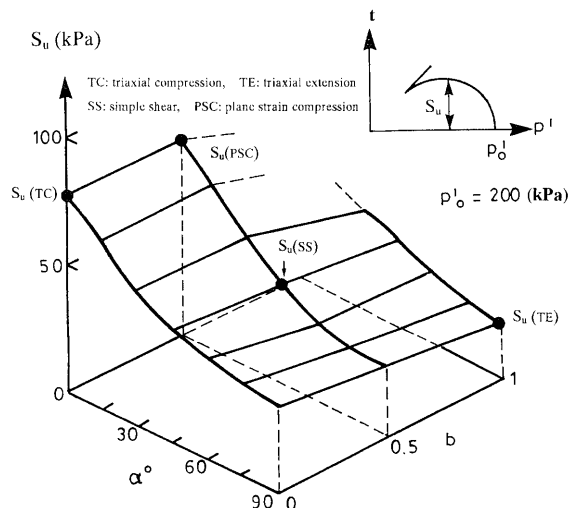


Fig. 17. Undrained peak strength from M-series tests plotted in (t, b, α) space

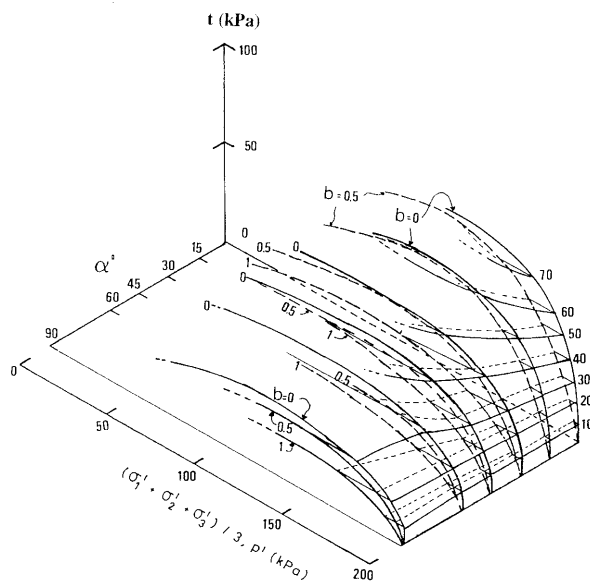


Fig. 18. Four dimensional undrained local boundary surface (4-D LBS) of isotropically consolidated loose Ham River sand

CONCLUSIONS

The initial undrained anisotropy, together with the effects of principal stress rotation of an isotropically consolidated loose Ham River sand has been investigated by performing three series of hollow cylinder tests that involved changes in t , p' , b and α .

- 1) The undrained response to monotonic loading was strongly affected by α , and was also influenced by the relative magnitude of intermediate principal stress as expressed by the b -value.
- 2) It was found that the sand's undrained anisotropy and cyclic response could be interpreted by invoking the concept of undrained Local Boundary Surface (LBS).
- 3) The effective stress paths developed in monotonic tests performed on normally consolidated samples at

constant values of b and α defined a four dimensional Local Boundary Surface that could not be crossed by any undrained effective stress path performed on similarly consolidated samples. Note that the surface governs behaviour only within contractant phase, where octahedral shear strains are generally well less than 1%.

4) The LBS could be visualized in (t, p', α) space as a family of superimposed 3-D shapes with the innermost surface corresponding to $b=1.0$ and the outermost to $b=0$.

5) The peak values of t available (in the contractant region) under the full range of b - α combinations could be expressed in a 3-D plot that gave another expression of the loose sand's initial anisotropy after isotropic consolidation.

6) Irrecoverable shear straining and reductions in p' could be developed through load cycling inside the LBS, with these occurring most readily during cyclic α rotation stages.

7) The 4-D LBS is useful in forecasting the conditions under which the loose sand would run-away or liquefy when tested under monotonic or cyclic conditions.

ACKNOWLEDGEMENTS

The experimental programme was financially supported by the UK Science and Engineering Research Council (SERC, now EPSRC). The authors are grateful for useful discussion given by Dr M. J. Symes and Professor A. Gens.

REFERENCES

- 1) Arthur, J. R. F. and Menzies, B. K. (1972): Inherent anisotropy in a sand, *Géotechnique*, **22** (1), 115-129.
- 2) Arthur, J. R. F. and Dunstan, T. (1977): Induced anisotropy in a sand, *Géotechnique*, **27** (1), 13-30.
- 3) Gens A. (1982): Stress-strain and strength characteristics of a low plasticity clay, *PhD thesis*, University of London.
- 4) Gens A. (1985): A state boundary surface for soils not obeying Rendulic's principle, *Proc. of 11th Int. Conf. on SMFE*, San Francisco, **2**, 473-476.
- 5) Hight, D. W., Symes, M. J. and Gens, A. (1983): The development of a new hollow cylinder apparatus for investigating the effects of principal stress rotation in sand, *Géotechnique*, **33** (4), 355-384.
- 6) Ishihara, K., Tatsuoka, F. and Yasuda, S. (1975): Undrained deformation and liquefaction of sand under cyclic shear stresses, *Soils and Foundations*, **15** (1), 29-44.
- 7) Jardine, R. J. (1992): Some observations on the kinematic nature of soil stiffness, *Soils and Foundations*, **32** (2), 111-124.
- 8) Jardine, R. J., Kuwano, R., Zdravkovic, L. and Thornton, C. (2001): Some fundamental aspects of the pre-failure behaviour of granular materials, Keynote Lecture, *Pre-failure Deformation Characteristics of Geomaterials (IS-Torino)*, Balkema, **2**, 1077-1111.
- 9) Kuwano, R. (1999): The stiffness and yielding anisotropy of sand, *PhD Thesis*, University of London.
- 10) Oda, M. (1972): Initial fabrics and their relations to mechanical properties of granular material, *Soils and Foundations*, **12** (1), 1-18.
- 11) Shibuya, S. (1985): Undrained behaviour of granular materials under principal stress rotation, *PhD Thesis*, University of London.
- 12) Shibuya, S. and Hight, D. W. (1987): A bounding surface for granular materials, *Soils and Foundations*, **27** (4), 123-136.

- 13) Shibuya, S. (1988): A servo system for hollow cylinder testing of soils, *Geotech. Testing J.*, **11** (2), 109-118.
- 14) Symes, M. J. and Burland, J. B. (1984): Determination of local displacements on soil samples, *Geotech. Testing J.*, **7** (2), 49-59.
- 15) Symes, M. J., Gens, A. and Hight, D. W. (1984): Undrained anisotropy and principal stress rotation in saturated sand, *Géotechnique*, **34** (1), 11-27.
- 16) Symes, M. J., Gens, A. and Hight, D. W. (1988): Drained principal stress rotation in saturated sand, *Géotechnique*, **38** (1), 59-81.
- 17) Tatsuoka, F. (1972): Fundamental study of deformation characteristics of sands using triaxial apparatus, *DEng Thesis*, University of Tokyo (in Japanese).
- 18) Yamada, Y. and Ishihara, K. (1979): Anisotropic deformation characteristics of sand under three dimensional stress conditions, *Soils and Foundations*, **21** (1), 97-109.
- 19) Zdravkovic, L. and Jardine, R. J. (2000): Undrained anisotropy of K_0 -consolidated silt, *Can. Geotech. J.*, **37**, 178-200.